

# Performance of the compatibilizing processes in Polystyrene/Ethylene-propylene-diene terpolymer/Polyamide6 (PS/EPDM/PA6): in-situ grafted versus pre-grafted compatibilizing method

Marzieh Alidadi-Shamsabadi<sup>1,\*</sup>, Ahmad Arefazar<sup>2</sup>, Shirin Shokoohi<sup>3</sup>, Mahnaz shahzamani<sup>1</sup>

<sup>1</sup> Chemistry & Chemical Engineering Technical Centre, Academic Centre for Education, Culture and Research (ACECR), Isfahan University of Technology branch, Isfahan, Iran

<sup>2</sup> Polymer Engineering Department, Amirkabir University of Technology, Tehran, Iran

<sup>3</sup> Chemical, Polymeric and Petrochemical Technology Development Research Division, Research Institute of Petroleum Industry, Tehran, Iran

\* Correspondence: [alidadi@acecr.ac.ir](mailto:alidadi@acecr.ac.ir)

Received: 12 March 2025, Accepted: 20 July 2025

DOI: 10.22063/POJ.2025.35682.1356

## ABSTRACT

In this work, the influence of compatibilizing method on the phase morphology, mechanical properties and rheological behavior of ternary blends based on polystyrene(PS) /ethylene-propylene-diene terpolymer(EPDM)/ polyamide6 (PA6) was investigated. Two different methods (including in-situ grafted and pre-grafted) were used to compatibilize PS/EPDM/PA6 ternary blends. In the first method, all reactive materials were mixed during mixing, but in the latter, modified EPDM was prepared first and then blended with other components. The chemical reactions occurred during blending followed by Attenuated Fourier Transform Spectroscopy (ATR-FTIR). Mechanical properties investigated by impact and tensile strength measurements. The phase microstructure was observed by Scanning electron spectroscopy (SEM) and the rheological behavior was carried out using a parallel plate rheometer in oscillatory mode. ATR-FTIR results confirmed the grafting and compatibilizing reactions. The morphology size of dispersed phase particles has dramatically changed by increasing EPDM-g-GMA content. The pre-grafted compatibilizing method has revealed finer microstructure than the other method. The modulus of all the ternary compatibilized blends has increased compared to PS/EPDM. In fact, the presence of PA6 introduces a new, more rigid phase in the blend. The pre-grafted compatibilizing method, which uses a compatibilizer content of less than 10 wt.%, is more effective than the in-situ grafted compatibilizing method. This approach results in a finer microstructure and enhanced impact strength. Additionally, it creates a more rigid interface, leading to greater elasticity, which manifests as a semi-plateau in the rheological behavior. In contrast, the in-situ grafted method produces more balanced mechanical properties overall.

**Keywords:** Ternary blend; grafting methods; morphological analysis; mechanical analysis; rheological analysis.

## INTRODUCTION

Melt mixing of two or more polymers is a common method widely used in the industry to obtain new high-performance materials at a relatively low cost compared to synthesizing new polymers [1-4]. The poor compatibility of binary or ternary blend components results in unsatisfactory mechanical properties, morphology, and interfacial interactions, highlighting the need for an effective compatibilizing method, either non-reactive or reactive [5-7]. Non-reactive methods involve adding a block or graft copolymer as a compatibilizer to enhance compatibility, although the improvement in properties is often modest [8]. Also, using nanoparticles as a non-reactive compatibilizer can enhance compatibility by localizing at the interface and controlling the microstructure [9]. On the other hand, reactive compatibilizing methods are more effective than non-reactive ones for improving compatibility and modifying the properties of blends by activating and forming compatibilizing copolymers during melt blending [10]. The reactive compatibilization commonly involves adding pre-grafted compatibilizers, while in-situ grafted is rarely used.

As a reactive pre-grafted compatibilizing method, Wang et al. [5] displayed that a multifunctional epoxide serves as a reactive compatibilizer for poly(lactic acid)/poly(butylene adipate-co-terephthalate) (PLA/PBAT) blends. The increasing compatibility and as a result improving mechanical properties can be attributed to the reaction of the epoxy group of reactive compatibilizer with the terminal carboxyl and hydroxyl groups of PLA and PBAT and form a large number of branched copolymers. Yang et al. [11] presented a novel compatibilizer featuring both reactive epoxide and maleic anhydride groups for the immiscible blend of poly (amide 11) and poly (L-lactic acid) (PA11/PLLA). By burying grafted PA11 chains in the PA11 phase and grafted PLLA chains in the PLLA phase, the compatibility of the PA11/PLLA blend was significantly enhanced, showcasing excellent ductility, outstanding impact strength, and high tensile strength. Seier et al. [12] investigated the effect of both a reactive and a non-reactive copolymer as compatibilizer for immiscible polypropylene (PP)–polystyrene (PS) blends with varying concentrations of PS. Nonreactive copolymers demonstrated a significant improvement in toughness and ductility, which was associated with optimal overall phase homogeneity. In contrast, the reactive copolymer at lower polystyrene (PS) concentrations exhibited a tensile impact strength that surpassed that of virgin polypropylene (PP). Filho et al. [13] presented three copolymers: Styrene-ethylene-propylene (SEP), styrene-ethylene-butylene-styrene (SEBS), and styrene-butadiene-styrene (SBS) as non-reactive compatibilizers for blends of polystyrene (PS) and acrylonitrile-butadiene-styrene (ABS) blends. SEP and SEBS demonstrated a better compatibilizing effect compared to SBS. In recent decades, the large number of researches have been conducted on the reactive compatibilization of polymer blends using the pre-grafted compatibilizing method. However, there have been relatively few studies on the in-situ grafted method for reactive compatibilization, although this method seems easier, more cost-effective, and time-efficient [2].

Polystyrene (PS) is a thermoplastic polymer which is simply processed, but presented brittle behavior at ambient temperature. Synthesis of high-impact PSs (HIPS) recommended as a solution, but HIPS

presented weak resistance against natural light radiation due to the probable photo degradation of polybutadiene (PB) segments. Thus, PB is replaced by ethylene-propylene-diene terpolymer (EPDM) in some researches and the PS/EPDM binary blends have been studied [14-17]. EPDM, as a rubber with excellent aging properties, has been used to enhance the impact strength of PS, but results in a reduction of other mechanical properties, such as tensile modulus.

In this study, EPDM rubber and PA6 were introduced to PS to improve both toughness and tensile characteristics. The PS/EPDM/PA6 ternary blend, proposed to address the aforementioned limitations of HIPS, has yet to be studied or evaluated [7]. The factors affecting the mechanical properties of this ternary blend (PS/EPDM/PA6) are investigated in our previous works [2, 7, 14, 18]. Mixing sequence, blend composition and viscosity ratio of the minor phases were studied and discussed in accordance with the morphology and mechanical properties of reactive compatibilized PS/EPDM/PA6 [2]. Modification of EPDM as a compatibilizer for this ternary blend were investigated previously [18]. However, there remains a question regarding how the modification of EPDM through processing of ternary blend as an in-situ grafted method compared to using pre-grafted EPDM as a reactive compatibilizer affects the properties of the ternary blend by enhancing compatibility between the EPDM and PA6 phases. Here, the effect of reactive compatibilization methods, pre-grafted and in-situ grafted, on the morphology, mechanical and rheological properties of this ternary blend are investigated. Accordingly, the effect of pre-grafted EPDM with glycidyl methacrylate (GMA) as a reactive compatibilizer were compared to the in-situ grafted ones and discussed.

## **EXPERIMENTAL**

### **Materials**

Materials used in this research were: (i) General purpose polystyrene (GPPS, Solarene® G-144) supplied by Hyundai Engineering Plastics (Korea), MFI: 8.5 g/10min @200°C & 5kg); (ii) Ethylene-propylene-diene terpolymer (EPDM, Kep270) supplied by Kumho Polychem (Korea), Mooney viscosity ML(1+4)125°C: 71 M, ethylene content: 57%, termonomer content: 4.5 ENB%, density: 0.86 g/cm<sup>3</sup>; (iii) Polyamide6 (PA6, Ultramid® B3S) supplied by BASF (Germany), MFI: 197.75 g/10min @275°C & 5kg as the low viscosity grade; (iv) Polyamide6 (PA6, PA 5010NH) supplied by Asia International (China), MFI: 168.10 g/10 min @ 275°C & 5kg as the medium viscosity grade; (v) Polyamide6 (PA6, Tecomid® NB40 NL E) supplied by eurotec-ep (Turkey), MFI: 139.22 g/10min @275°C & 5kg as the high viscosity grade; (vi) Glycidylmethacrylate monomer (GMA) supplied by Aldrich Chemical Co. (Japan), 97 and (vii) Dicumyl peroxide (DCP) supplied by Merck Millipore (Germany), 98.

### **Blend Preparation**

All ternary blend samples listed in Table 1, were prepared at 220°C in an internal batch-mixer (Brabender GmbH, Germany) with rotor speed 120 rpm for overall mixing time [2, 19]. Before mixing, all components were dried for 24 h at 80°C to remove moisture. Two different methods were used to compatibilize PS/EPDM/PA6 ternary blends. In the first compatibilizing method, in-situ grafted method, half of the weighed EPDM was cut into small, flaky pieces and then physically impregnated with DCP and GMA. The mixture was placed in a closed container for 20 minutes at ambient temperature to allow the physical absorption of the active components onto the surface of the EPDM. The composition containing EPDM, DCP and GMA acts as an reactive compatibilizer during the final melt blending of the ternary blend [2]. After that, all components were blended together using the internal mixer for 10 min. In the second compatibilizing method, pre-grafted method, the modified EPDM (EPDM-g-GMA) was prepared by melt free radical grafting method [18]. Then, all components, including EPDM-g-GMA, were blended together using the internal mixer for 10 min.

**Table 1:** Composition of the prepared samples.

Compatibilizing method	Sample code	PS (%wt.)	PA6 (%wt.)	EPDM (%wt.)	Compatibilizer				$\frac{EPDM-g-GMA}{EPDM}$
					EPDM-g-GMA (%wt.)	EPDM (%wt.)	DCP* (hpr)	GMA* (hpr)	
---	PS/EPDM	70	---	30	---	---	---	---	---
---	B0	70	15	15	0	0	0	0	$\frac{0}{3}$
In-situ grafted	B5-C	70	15	10	0	5	0.15	3	$\frac{1}{2}$
	B7.5-C	70	15	7.5	0	7.5	0.15	3	$\frac{1}{1}$
	B10-C	70	15	5	0	10	0.15	3	$\frac{1}{2}$
	B15-C	70	15	0	0	15	0.15	3	$\frac{1}{3}$
Pre-grafted	B5	70	15	10	5	0	0	0	$\frac{1}{2}$
	B7.5	70	15	7.5	7.5	0	0	0	$\frac{1}{1}$
	B10	70	15	5	10	0	0	0	$\frac{2}{1}$
	B15	70	15	0	15	0	0	0	$\frac{3}{0}$

\*based on the virgin EPDM in the compatibilizer

## Characterization

### ATR-FTIR Analysis

Samples B5-C, B7.5-C, B15-C, B5, B7.5 and B15 were typically characterized with Attenuated Total Reflection-Fourier Transform Infrared (ATR-FTIR) spectroscope (Bruker Vertex70, USA). Moreover, each sample was also analyzed after keeping immersed in formic acid for one week to remove unreacted PA6.

### Mechanical Analysis

Standard specimens for tensile and impact strength tests were machined from sheets compression-molded at 240°C. Tensile tests measuring stress-strain variations under load were conducted by Galdabini testing machine (Italy) with crosshead speed of 1 mm/min at room temperature according to ASTM D638. Un-notched Izod impact tests were carried out using Ueshima impact tester machine (Japan) according to ASTM D4812.

#### *Morphological Analysis*

A Philips (XL30, Netherlands) scanning electron microscope (SEM) was used to observe the phase microstructure of ternary blends. Fracture surface of impact tests was etched by *n*-Heptane to remove EPDM phase. Etched surfaces were then coated with a thin layer of gold by BAL-TEC SCD 005 sputter coater.

#### *Rheological Analysis*

The rheology measurements were carried out using a MCR302 rheometer (Anton-Paar GmbH, Austria) using a parallel plate configuration in oscillatory mode. The parallel plate's diameter was 25 mm, with a gap distance 1 mm. A strain of 1% was applied that is within the linear viscoelastic region. Sweep in the range of 0.01-1000 s<sup>-1</sup> were performed from high to low frequencies. The rheological behavior of studied ternary blends were conducted at the processing temperature (220°C).

## **RESULTS AND DISCUSSION**

### **ATR-FTIR Analysis**

To confirm the occurrence of GMA monomers grafting onto polymer backbones (as illustrated in Figure 1(a) and (b)) and the compatibilization reaction (as illustrated in Figure 1(c)) between the epoxy groups of the grafted polymer backbones and the primary amine groups of PA6 chains, ATR-FTIR analysis was performed on the studied samples.

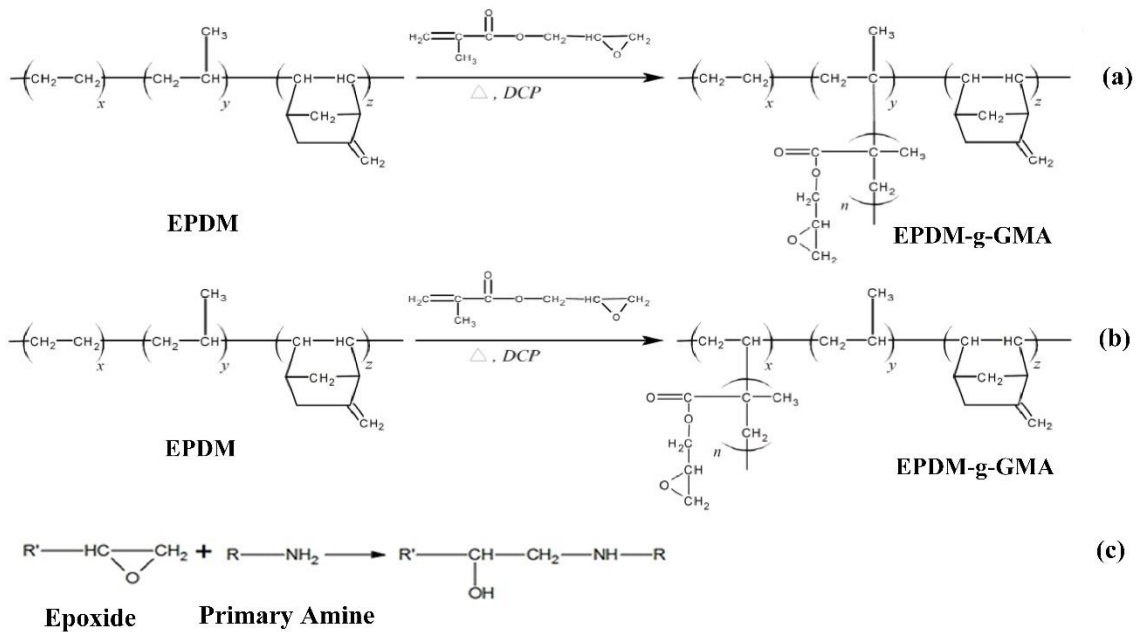


**Figure 1.** Schematic reaction between (a), (b) EPDM backbone and GMA, (c) GMA grafted on the polymer backbone and amine end groups.

As shown in Figure 2, every ATR-FTIR spectrum contains two essential peak categories. The first peak occurs at  $1740\text{ cm}^{-1}$  and can be attributed to the carbonyl group ( $\text{C}=\text{O}$ ) resulting from glycidyl methacrylate (GMA) grafting onto the EPDM backbone [2, 7, 20]. This is observed in both pre-grafted and in-situ grafted compatibilizing methods. The presence of the mentioned peak confirms the occurrence of a grafting reaction in both methods.

As shown in Figure 2, another peak category is observed in the range of  $3000\text{-}3400\text{ cm}^{-1}$ , where three distinct peaks are identified. The peaks observed at  $3000\text{-}3100\text{ cm}^{-1}$  (at  $3024$  and  $3061\text{ cm}^{-1}$ ) and  $3303\text{ cm}^{-1}$  are attributed to primary (a double band) and secondary (a single band) amine groups of PA6, respectively [7]. Interestingly, the peaks mentioned earlier are still present for all etch samples. This observation supports the occurrence of a compatibilization reaction between the epoxy groups of GMA (grafted onto polymer backbones) and the amine groups of PA6, as illustrated in Figure 1 [2].

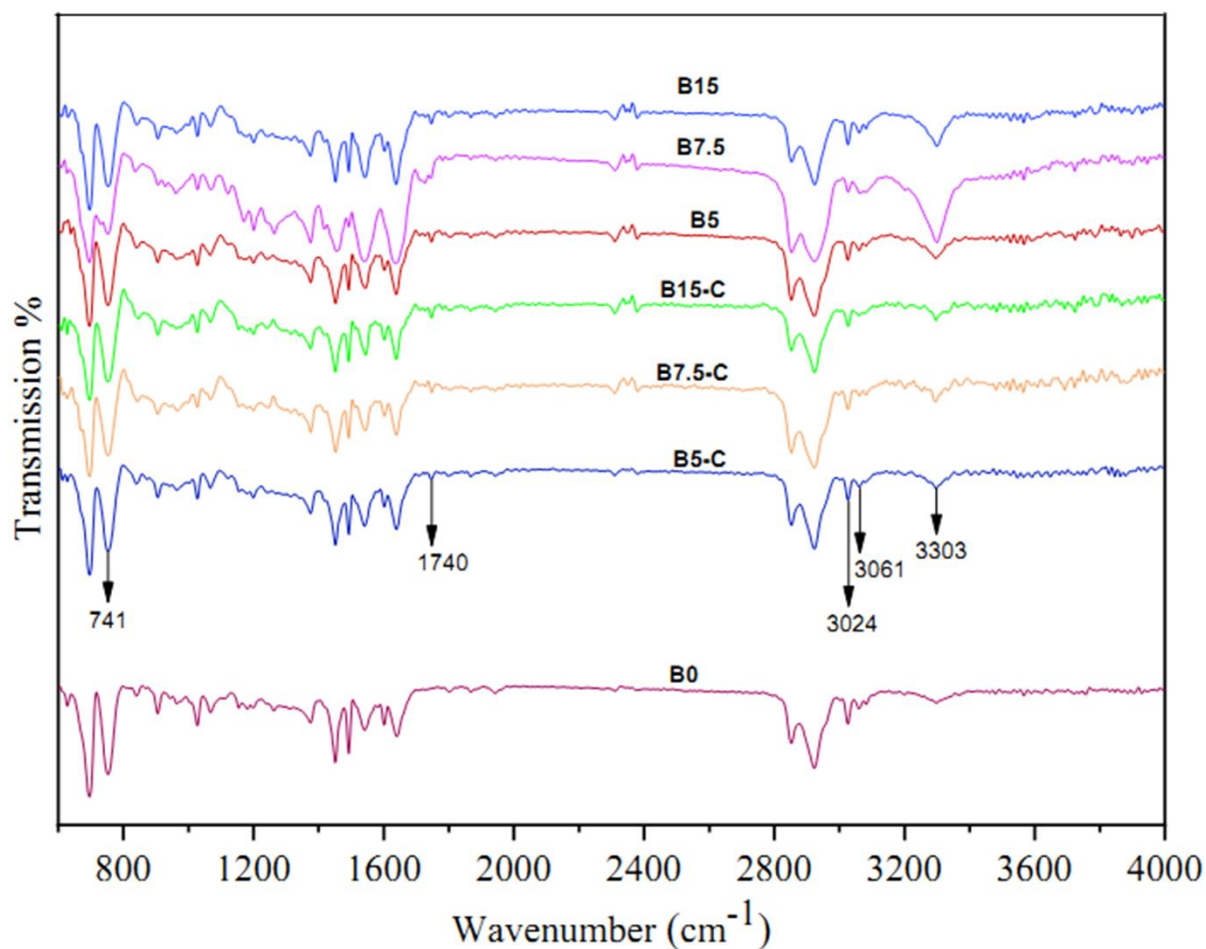


**Figure 2.** ATR-FTIR analysis for seven random samples after removing un-reacted PA6.

### Morphological Analysis

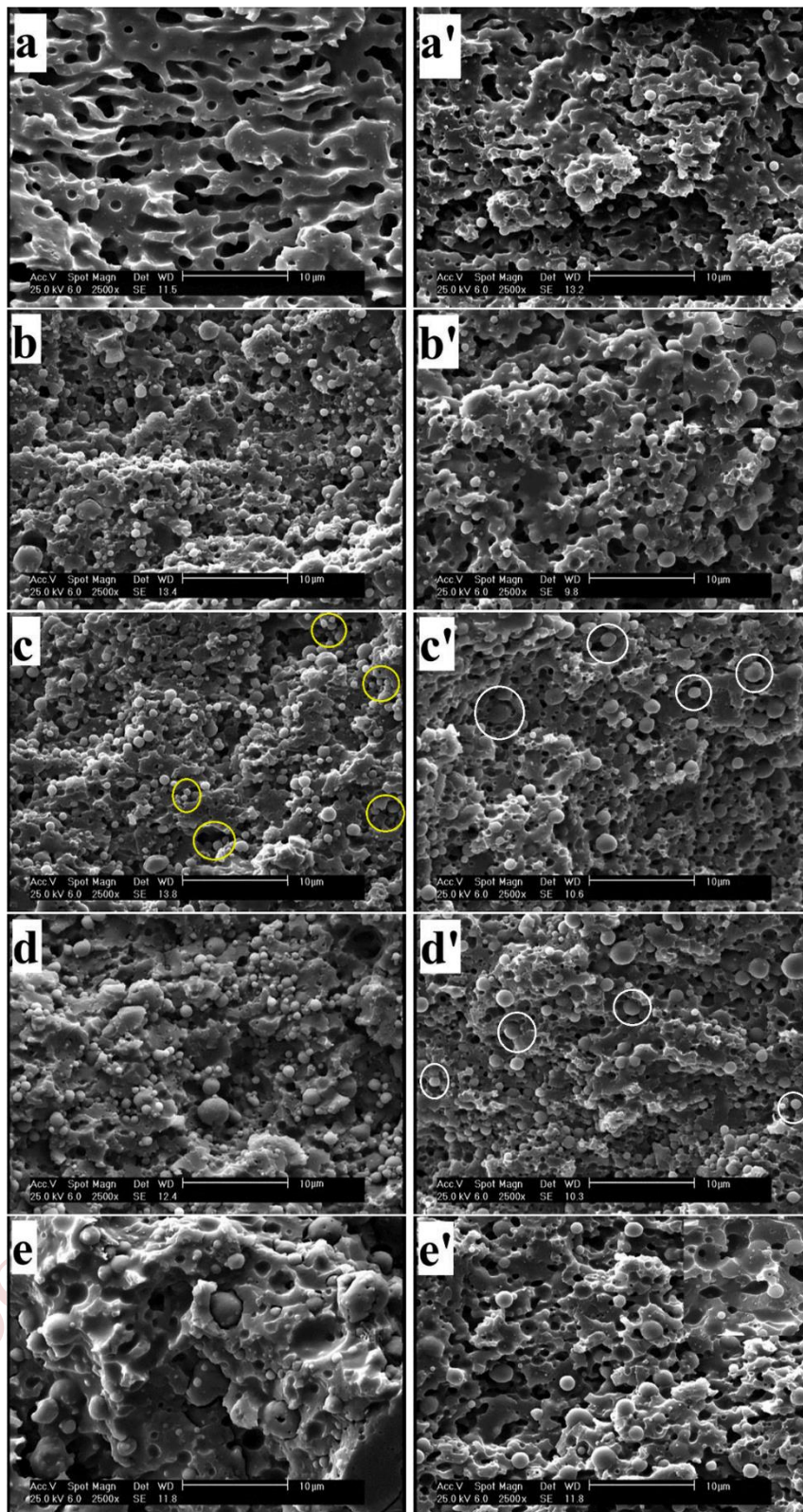
The SEM micrograph of all prepared ternary blends presented in Figure 3. As shown, the type of morphology and the size/number of dispersed particles presented an obvious change with increasing compatibilizer in two methods. It should be noted that the black holes and white cores represent rubber phase and PA6 droplets, respectively (Figure 3).

Figure 3a clearly shown that the morphology of PS/EPDM binary blend has appeared in the form of the large stretched non-spherical EPDM particles through PS matrix phase. By replacing half of the EPDM phase with PA6 as a hard phase, EPDM droplets have appeared smaller and closer to core shape, while the ternary blend microstructure has changed to separated dispersed morphology (Figure 3a). In fact, by decreasing EPDM content in ternary blend, the rubber coalescence becomes weaker resulting in smaller EPDM droplet [21]. On the other hand, the high PA6/EPDM interfacial tension (6.67 mN/m) leading rubber droplets to core-shell morphology decreasing the interfacial tension with PA6 phase [7].

The results presented in Figure 3(a', b', c', d', and e'), for in-situ grafted compatibilized samples, confirms changes in the morphology, the size and the number of dispersed phase particles with increasing compatibilizer from 0 (B0) to 15 %wt (B15-C). With gradual increase in compatibilizer, from 0-10 %wt., separated dispersed morphology weakened and simultaneously partial core-shell morphology (PA6 as core surrounded by EPDM as shell) got stronger (Marked with white circles). In fact, by adding the compatibilizer in the uncompatibilized blend (B0), the interfacial tension between rubber phase and PA6 reduced due to interfacial tensions as a function of interfacial reactions and activities changed by altering the EPDM-g-GMA/EPDM ratio [22] . Therefore, PA6 gradually has migrated from PS bulk towards rubber particles and as a result of epoxy-amine reaction between two dispersed phases, partial core-shells were gradually formed [21] . Improved compatibility with the finest PA6 cores and rubber dispersed particles have appeared in 10 wt. % compatibilizer (B10-C). The results presented that the morphology has gotten coarse by adding compatibilizer content more than 10 %wt [23, 24].

As seen in Figure 3(a', b, c, d, and e), the type of morphology and the size of dispersed phase particles has dramatically changed by increasing in EPDM-g-GMA content for the pre-grafted samples. Addition of only 5 wt. % compatibilizer leading to a drastic change in the morphology from separated dispersed to partial core-shell and rubber dispersed in the form of fine spherical particles (Figure 3b). The epoxy-amine reaction followed by reducing interfacial tension between rubbery and PA6 phases, moving PA6 particles from PS bulk towards rubbery phase and partially surrounded by rubbery phase. By using 7.5 wt. % compatibilizer (B7.5), partial multicore-shell morphology (Marked with yellow circles) with the finest and the most numerous PA6 cores has appeared as seen in similar studies of ternary blends with rubbery and rigid dispersed phases. [21-24] (Figure 3(c)).

As seen with increasing the compatibilizer amount, changes in the type and size of the microstructure is much more severe in the pre-grafted method compared to the in-situ grafted method. In the pre-grafted method, the graft reaction of GMA on the rubber chain has already been performed allowing the epoxy-amine reaction and intensification during the mixing. Therefore, better compatibilization, finer dispersed particles and microstructure changes can be resulted with increasing the compatibilizer amount. On the other hand, the equal mixing time for in-situ grafted method is limited for compatibilization and slight changes in the microstructure seen with the increase in the compatibilizer amount. This is because of that rubber modification and epoxy-amine reactions must occur simultaneously and need more time in this method.



**Figure 3.** SEM micrographs of etched surface of (a) PS/EPDM (70/30); (a') B0; (b) B5; (b') B5-C; (c) B7.5; (c') B7.5-C; (d) B10; (d') B10-C; (e) B15; (e') B15-C.

## Mechanical Analysis

The interactions that might be established between the blends constituents can affect the microstructure, which in turn determine the mechanical properties. Thus, the mechanical properties, including tensile and impact strength properties, for the samples prepared by both methods have been measured as observed in Table 2. Also, the stress-strain curves from the tensile test are shown in Figure 4.

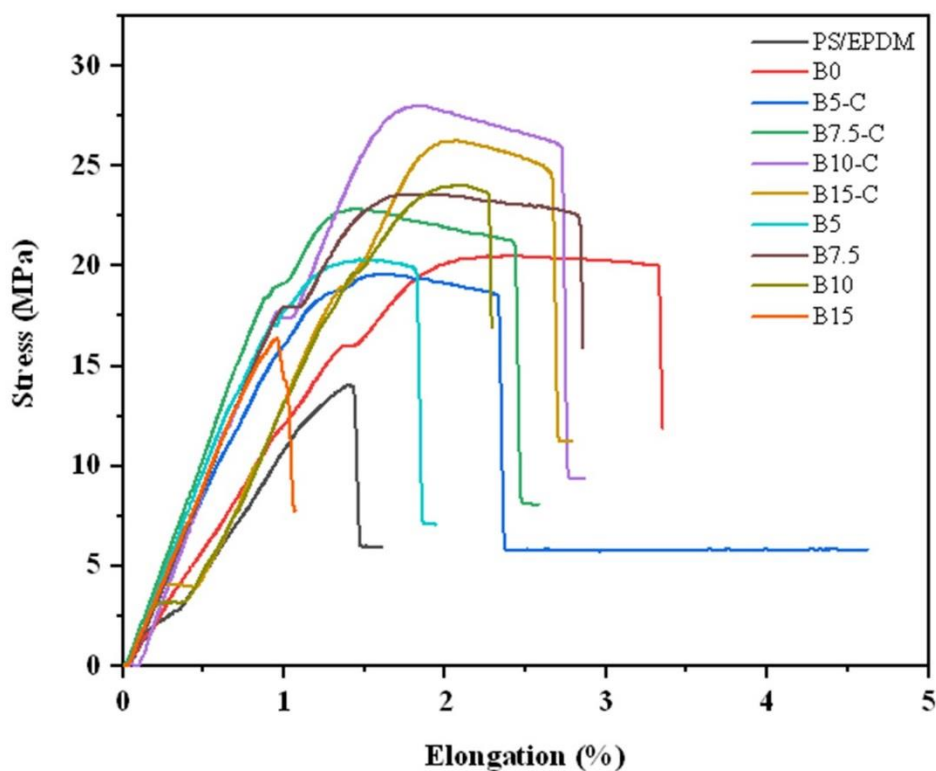


**Figure 4.** Stress-strain curves of all prepared blends.

**Table 2:** Tensile and impact strength properties of compatibilized samples.

Compatibilization method	Sample Code	Tensile modulus (MPa)	yield strength (MPa)	Impact Strength (J/m)
In-Situ grafted	PS	3363±24	----	4.0±5.3
	PS/EPDM	1314±18	12.1±9.7	84.4±8.0
	B0	1674±15	19.0±4.0	7.0±0.6
	B5-C	1932±16	22.0±2.7	14.1±0.03
	B7.5-C	1891±23	24.3±9.3	16.0±7.9
	B10-C	1835±25	27.0±2.6	12.0±1.7
	B15-C	2172±13	26.2±1.9	25.8±12.1
	B5	1986±22	20.0±1.2	28.0±1.8
	B7.5	1958±21	23.0±7.4	31.0±2.9
	B10	2018±12	23.0±0.7	32.0±7.7
Pre-grafted	B15	2203±19	16.0±6.5	20.1±4.0

Tensile modulus of PS/EPDM binary blend was observed to decrease about 63% compared to pure PS. As the modulus of the blends is strongly dependent on the stiffness of the blend phases, this reduction of the modulus can be attributed to the addition of a soft rubber phase to the rigid PS phase [23-25]. On the other hands, modulus and yield stress of all the ternary blend samples increased compared to PS/EPDM binary blends. This phenomenon can be attributed to the replacement 50 wt.% of the soft rubber phase with the rigid PA6 phase [26]. Among all ternary blends, the incompatible ternary blend (B0) showed the lowest modulus and yield stress which is ascribed to the presence of large stretching droplets of the soft rubber phase within the continuous PS phase [24]. The yield stress drop is attributed to the weak interfacial adhesion between blend components, especially the rubber phase with PS and PA6 [21, 24].

Tensile modulus also increased by increasing the compatibilizer content up to 5wt. % for the in-situ grafted compatibilized blends (B5-C). Since the modulus is strongly dependent on the rubber microstructure, reduction of rubber content in the continuous phase would be responsible for the reduction in interfacial strain and the consequent modulus increase [23, 26]. Furthermore, with an increase in compatibilizer content to 10 wt. % (B10-C), tensile modulus drops to its minimum value (1835 MPa). This is in accordance with SEM micrographs (Figure 3) in which fewer rigid PA6 dispersed phase particles and more small-sized partial core-shells are observed (0.598  $\mu\text{m}$ ) [24, 26]. According to Figure 3(e)', at high compatibilizer contents (15% wt.), due to the decrease in core-shell partials number and an increase in rigid PA6 core size (1.412  $\mu\text{m}$ ), the modulus has suddenly increased under PA6 reinforcement effect [26]. In the in-situ grafted method, by increasing the compatibilizer content from 0% (B0) to 15 wt. % (B10-C), yield stress values initially increased to a maximum value at 10% (27.2 MPa) followed by a decreasing trend. Yield stress is controlled by several factors, such as volume fraction of blend components, particle average diameter and its distribution as well as the interfacial adhesion [32, 34]. According to the SEM micrographs in Figure 3 by increasing the compatibilizer content up to 10wt.%, the dispersed rubber particles and PA6 hard cores size reduced to their minimum, indicating an improvement in interfacial adhesion. This is in accordance with the initial increase in yield stress [21]. In fact, an increase in interfacial interactions has improved the yield stress by reducing polymer chain segment mobility near the compatibilizer [27]. The slight decrease in yield stress could be attributed to the higher contents of the compatibilizer (B15-C) and the dispersed rubber particles enlargement.

Similar trend was observed in the tensile modulus of samples prepared through pre-grafted method, which is confirmed with the decrease in the number of dispersed rigid PA6 phase particles, increase in the number of core-shell particles and a decrease in the size of rigid PA6 core at high compatibilizer contents. The minimum modulus (1958 MPa) was obtained for B7.5. In Figure 3, it is understood that in sample B7.5 the core-shell partial particles have reached to their maximum number and the hard PA6 cores are at their minimum size. this is the main reason for the minimum modulus value [26].

Changes in yield stress by increasing the composition of EPDM-G-GMA compatibilizer showed a similar trend independent of the preparation method. The highest yield stress value was measured for sample B7.5 which contains partial core-shells with the smallest rigid PA6 in Figure 3 propounding the highest interfacial adhesion confirmed by the utmost epoxy-amine reactions progress evidenced in Figure 3 [23]. At equal contents of compatibilizer, the yield strength obtained through in-situ grafted method is higher than the pre-grafted method; whereas epoxy-amine reactions progress and the consequent interfacial adhesion between blend components were observed to be higher in the in-situ grafted compatibilizing method, according to Figure 3. This could be attributed to the gel phase present in EPDM-g-GMA samples (as measured in previous work for EPDM-g-GMA and reported to be 2.2 wt. % [18]) involved in the pre-grafted method. These gel-like domains, resulting from the cross-linking reactions in the EPDM rubber modification process using GMA monomer and DCP initiator, have a high modulus. The weak adhesion between gel phase and the blend components leads to the beginning of the yielding phenomenon at lower stress values. Accordingly, as in Table 2, the modulus values are also higher for equal percentage combinations in the pre-grafted method compared to the in-situ grafted method.

The Izod impact strength of the compatibilized samples prepared by both in-situ and pre-grafted methods, without any cracks, are measured and reported in Table 2. Impact strength of PS/EPDM blend is almost twice that of pure PS. It is clear that adding EPDM rubber to the brittle PS continuous phase increases its impact resistance since rubber has a strong toughening effect [23-25]. In fact EPDM acts as an impact modifier [25]. Interestingly, sample B0 showed an impact strength lower than the binary blend. This could be attributed to replacement of EPDM rubber phase half content with hard PA6 phase which are isolately dispersed in the continuous PS phase. It is clear that in both compatibilizing methods, among all ternary blends, the blend without compatibilizer B0 had the lowest impact strength. The weak interfacial interaction between the blend phases [24] and the rigid PA6 domains dispersed in PS might be responsible for this behavior [26].

According the Table 2, in both compatibilizing methods studied here, by increasing the compatibilizer composition, the initial increases in impact strength is followed by a significant drop about 25% of the maximum value of impact strength. In fact, in both methods, increasing the amount of compatibilizer has improved the interfacial interactions due to the epoxy-amine reactions progress. Thereupon, PA6 hard phase dispersed particles have left the continuous phase forming new partial core-shells. Since rigid dispersed particles and composite droplets, respectively, have a negative and positive effect on impact strength; an improvement is expected in the impact strength [24]. The maximum impact strength for the in-situ grafted and pre-grafted compatibilizing method has appeared in 10 wt. % of compatibilizer for sample B10-C (32.7 J/m) and 7.5wt. % for sample B7.5 (16.7 J/m), respectively. At higher compatibilizer contents, enlargement of isolately dispersed particles (in-situ grafted method) and core-shells (pre-grafted method) favors stress concentration and reduces the impact strength [23, 26].

## Rheological Analysis

In order to provide information about the rheological behavior of the blends, a shear rheometric test with decreasing frequency was performed at a temperature of 220°C for selected samples. Factors such as percentage composition, compatibility, microstructure, and interfacial contact between phases affect the rheological behavior of polymer blends. However, due to the large number of interactions and chemical and physical reactions that occur in the mixture, a complete description of the rheological behavior of polymer blends is difficult [28, 29]. The storage modulus ( $G'$ ) as a function of frequency ( $\omega$ ) is shown in Figure 5.

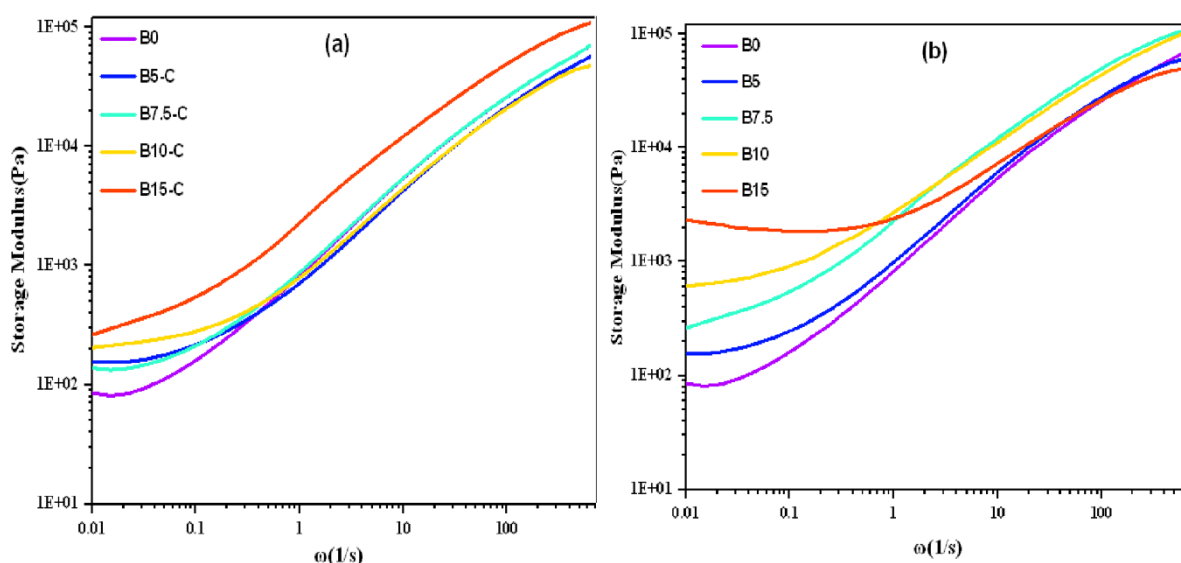


**Figure 5.** Changes of storage modulus against frequency for samples compatibilized by (a) in-situ grafted and (b) pre-grafted methods.

As can be seen in Figure 5, the storage modulus at low frequencies for all ternary blends compatibilized by both in-situ grafted and pre-grafted methods, was higher than the incompatible B0 ternary blend. As we know, the storage modulus is related to the elastic characteristic of blends and is responsible for reversible processes. Therefore, any phenomenon that leads to an increase in blend elasticity increases the storage modulus [28, 30]. In fact, adding a compatibilizer to the blend has led to a decrease in interfacial tensions and an increase in the interactions between the rubber phase and two PS and PA6 phases. Also, from a chemical point of view, adding a compatibilizer improves interfacial adhesion at the interface of two phases of rubber and PA6, which is caused by the epoxy-amine chemical reaction between epoxy functional groups and primary amine groups at interface of these two phases, confirmed by ATR-FTIR present in Figure 2. The sum of these events has led to the hardening of the interfaces and increased droplet resistance against deformation. On the other hand, polymer chain entanglement on each other under shear stress has made them harder and increased elasticity and

consequently increased storage modulus at low frequencies compared to incompatible blends [28, 31]. As can be seen in Figure 5, this phenomenon intensifies with increasing the compatibilizer content, which is manifested as an increase in the storage modulus of low frequencies with increasing the compatibilizer content.

It is clear from Figure 5(b), that as the compatibilizer increases, the storage modulus diagram at low frequencies appears as a plateau. This behavior indicates the presence of multi-phase blends with solid-like behavior. In fact, these reactions and interactions have limited the movement of chains by opening them from each other. On the other hand, the presence of gel resulting from rubber cross-linking reaction has also trapped rubber chains and contributed to the doubling of elasticity in the blend. These factors have caused the deviation in the behavior of the blend under shear from the liquid-like state to solid-like behavior at low frequencies. It should be noted that composite droplets formed during compatibilizer addition are also resistant to deformation and their elasticity appears as a plateau at intermediate frequencies, but in the studied blend, the slight difference in elasticity between droplets and chains has caused droplet elasticity to appear at low frequencies as well. By comparing Figure 5(a, b) it is clear that that plateau formation in the pre-grafted method, especially for samples B10 and B15, is much more severe than the in-situ grafted method. The amount of gel in compatibilized samples using the pre-grafted method and the interactions in the interface are higher than the in-situ grafted method that it has led to even higher elasticity and more severe solid-like behavior in the pre-grafted method compared to the in-situ grafted method. It can be confidently stated that severe plateau formation for sample B15 is mostly due to the presence of composite droplets with very large PA6 core (1.957  $\mu$ ), as evident from Figure 3(e) These large droplets have a high contact surface area with continuous phase, which results in higher elasticity and wider plateau formation for sample B15 compared to other samples.

The Cole-Cole curve, which shows the changes in  $\eta''$  versus  $\eta'$ , is recognized as the best reference for investigating the relationship between compatibility, phase microstructure and rheological behavior of polymer blends [28, 32].

The Cole-Cole curve of the blends prepared by two methods, in-situ grafted and pre-grafted, is presented in Figure 6. The relaxation phenomenon appears as an arc and tail on the Cole-Cole curve. Therefore, for homogeneous blends, only one arc appears, and for heterogeneous blends depending on the number and separation of phases, one or two arcs followed by a tail appear. While the Cole-Cole curve generally exhibits two relaxation mechanisms for multiphase blends [28].

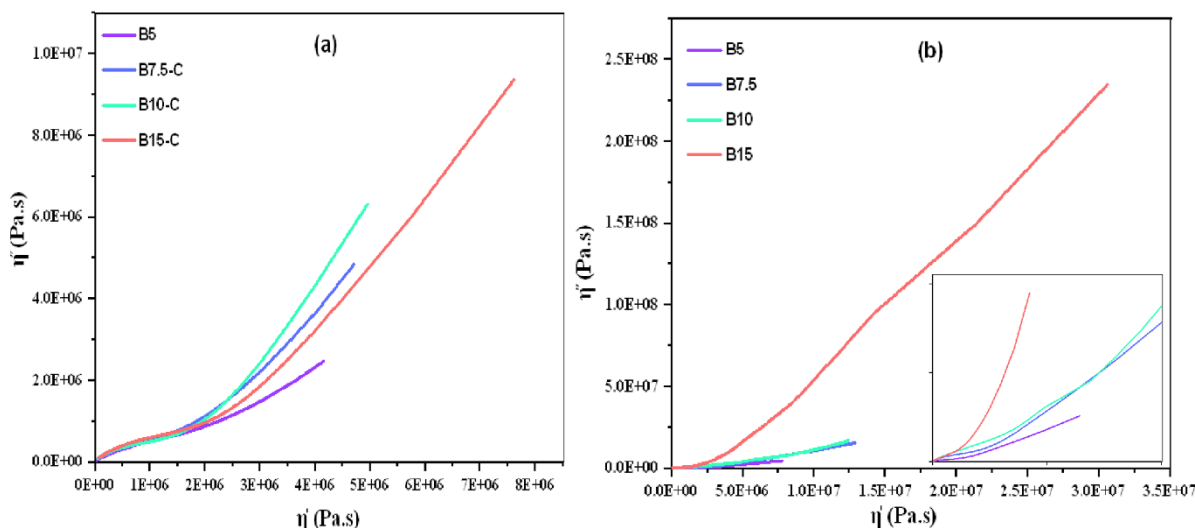


**Figure 6.** Cole-cole plot for compatibilized sample prepared by methods (a) in-situ grafted and (b) pre-grafted methods.

In Figure 6(a), it can be observed that for all the compatible blends prepared by in-situ grafted method, the curve appears as an arc and a linear sequence. The first arc, which is related to high frequencies, belongs to the relaxation of the continuous phase of PS, which appeared in the curve of all the samples [28]. The linear sequence indicates the interactions created between dispersed phases due to the addition of compatibilizer to the blends, which caused the dispersed phases to undergo uninterrupted and continuous relaxation mechanism one after another [32]. Interestingly, the length of the linear sequence has increased by compatibilizer increase. In fact, increasing the interaction between phases with increasing compatibilizer has made it more difficult for chains under shear stress to move and slowed down the relaxation mechanism. As a result, longer linear sequences have appeared as a sign of longer relaxation time [28]. The presence of very large composite droplets containing a high resistance core with an average diameter of  $1.412 \mu\text{m}$  has greatly increased the elasticity of sample B15-C and led to severe slowing down of relaxation and occurrence of very long linear sequences in this sample. Of course, higher gel content and consequently trapped chains in gel have also affected slowing down relaxation phenomenon at high compatibilizer concentrations.

It is obvious in Figure 6(b) that in the pre-grafted compatibilizing method, the Cole-Cole curve for samples B5 and B7.5 has appeared as an arc and a linear tail, which is due to the increase of interactions in B7.5 compared to the B5 sample, resulting in a slower relaxation mechanism and a longer linear tail. It is interesting that the Cole-Cole curve for the 10wt. % compatibilizer in B10 and 15wt. % compatibilizer for B15 appeared as two arcs and a linear tail. The occurrence of an arc and tail at low frequencies followed by the continuous phase relaxation arc indicates that after the occurrence of continuous phase relaxation mechanism at short times, despite the higher compatibilizer percentage,

compared to samples B5 and B7.5, the blend has undergone interruptedly and discontinuously through two relaxation mechanisms. In fact, due to the presence of larger and more elastic composite droplets in these two samples compared to other samples and also the presence of a higher percentage of gel compared to other samples, relaxation occurred through two separate mechanisms first for droplets (arc) at shorter times and then for chains (linear tail) at longer times. The occurrence of relaxation through more than one mechanism can indicate the severe heterogeneity in the blend [28]. It can be said that the high amount of gel in sample B15 has greatly increased elasticity and significantly slowed down chain relaxation mechanism. This phenomenon has led to a longer Cole-Cole curve for this sample compared to other blends.

## CONCLUSIONS

In this study, the effects of pre-grafted and in-situ grafted methods on the morphology, mechanical properties and rheological behavior of PS/EPDM/PA6 ternary blends were investigated. The samples were compatibilized through different compatibilizing methods: in-situ grafted and pre-grafted. Presence of carbonyl ester group (C=O) resulting from GMA grafting on EPDM backbone were followed in both blending methods. The results indicated that the reaction has been performed during mixing ternary blend for in-situ one. The primary and secondary peaks of amine groups correlated to PA6 were also recognized and confirmed epoxy-amine reaction.

As seen with increasing the amount of compatibilizer, changes in the type and size of the microstructure is much more severe in the pre-grafted compared to the in-situ grafted method. In the pre-grafted, the graft reaction of GMA on the rubber chain has already been performed, allowing the epoxy-amine reaction to occur and intensify during the mixing time resulting in finer dispersed particles, and microstructure changes.

It was observed that both compatibilizing methods lead to improved mechanical properties compared to the blends without compatibilizer, which is attributed to the improvement of interfacial adhesion between phases which result in better stress transfer from the dispersed phase to the continuous phase. Overall, in-situ grafted compatibilized samples shown the most balanced properties with 10wt. % compatibilizer resulting an improvement in tensile modulus, yield stress and impact strength, compared to non-compatibilized blend. Thus, it is clear that the in-situ grafted method is more efficient than the pre-grafted method for improving the mechanical properties. The obtained results also confirmed the rheological behavior of this ternary blend.

## REFERENCES

1. Afsari B, Razavi Aghjeh MK, Hasanpour M (2020) Evolution of morphology and morphology stability in PP/PA6/EPDM-g-MA reactive ternary blends using viscoelastic measurements. *Rheo Acta* 59: 399-414 [\[CrossRef\]](#)
2. Alidadi-Shamsabadi M, Arefazar A, Shokoohi S (2020) Response surface analysis of PS/EPDM/PA6 ternary blends: Effect of mixing sequence, composition, and viscosity ratio on the mechanical properties. *J Vinyl Addit Technol* 26: 282-290 [\[CrossRef\]](#)
3. Hasanpour M, Mazidi MM, Aghjeh MKR (2019) The effect of rubber functionality on the phase morphology, mechanical performance and toughening mechanisms of highly toughened PP/PA6/EPDM ternary blends. *Polym Test* 79: 106018 [\[CrossRef\]](#)
4. Wang D, Li Y, Xie X, Guo B (2011) Compatibilization and morphology development of immiscible ternary polymer blends. *Polymer* 52: 191-200 [\[CrossRef\]](#)
5. Wang X, Peng S, Chen H, Yu X, Zhao X (2019) Mechanical properties, rheological behaviors, and phase morphologies of high-toughness PLA/PBAT blends by in-situ reactive compatibilization. *Compos B: Eng* 173: 107028 [\[CrossRef\]](#)
6. Lin T, Padilla-Vélez O, Kaewdeewong P, LaPointe AM, Coates GW, Eagan JM (2024) Advances in nonreactive polymer compatibilizers for commodity polyolefin blends. *Chem Rev* 124: 9609-9632 [\[CrossRef\]](#)
7. Alidadi-Shamsabadi M, Shokoohi S, Shahzamani M, Abbasian-Peykani H (2025) Evaluation of photo-aging changes in mechanical properties of HIPS, PS-based binary and compatibilized ternary blends. *Polyolefins J* 12: 45-52 [\[CrossRef\]](#)
8. Belyamani I, Bourdon S, Brossard J, Cauret L, Fontaine L, Montembault V, Maris J (2024) A sustainable approach toward mechanical recycling unsortable post-consumer WEEE: Reactive and non-reactive compatibilization. *Waste Manage* 178: 301-310 [\[CrossRef\]](#)
9. Hu J, Hao X, Ning N, Yu B, Tian M (2023) Reactive Janus particle compatibilizer with adjustable structure and optimal interface location for compatibilization of highly immiscible polymer blends. *ACS Appl Mater Interfaces* 15: 23963-23970 [\[CrossRef\]](#)
10. Fredi G, Dorigato A (2024) Compatibilization of biopolymer blends: A review. *Adv Ind Engg Polym Res* 7: 373-404 [\[CrossRef\]](#)
11. Yang X, Wang H, Chen J, Fu Z, Zhao X, Li Y (2019) Copolymers containing two types of reactive groups: New compatibilizer for immiscible PLLA/PA11 polymer blends. *Polymer* 177: 139-148 [\[CrossRef\]](#)
12. Seier M, Stanic S, Koch T, Archodoulaki V (2020) Effect of different compatibilization systems on the rheological, mechanical and morphological properties of polypropylene/polystyrene blends. *Polymers* 12: 2335 [\[CrossRef\]](#)

13. de Sousa Filho VA, de Albuquerque Filho MA, de Alencar Lira MC, Pedrosa TC, da Fonseca LS, Araújo SS, Henrique MA, da Silva Barbosa Ferreira E, Araújo EM, Luna CBB (2023) Efficiency assessment of the SEBS, SEP, and SBS copolymers in the compatibilization of the PS/ABS blend. *J Polym Res* 30: 425 [\[CrossRef\]](#)
14. Alidadi-Shamsabadi M, Shokoohi S (2021) Melt free-radical grafting of glycidyl methacrylate (GMA) onto epdm backbone and effect of EPDM-g-GMA on the morphology and mechanical properties of PS/EPDM/PA6 ternary blends. *Polyolefins J* 8: 1-9 [\[CrossRef\]](#)
15. Fang Z, Guo Z, Zha L (2004) Toughening of polystyrene with ethylene-propylene-diene terpolymer (EPDM) compatibilized by styrene-butadiene-styrene block copolymer (SBS). *Macromol Mater Eng* 289: 743-748 [\[CrossRef\]](#)
16. Li J, Guo S, Slezák R, Hausnerová B (2005) In situ compatibilization of PS/EPDM Blends during ultrasonic extrusion. *Macromol Chem Phys* 206: 2429-2439 [\[CrossRef\]](#)
17. Thomas SP (2022) Polystyrene-based composites and their toughening mechanisms. In: *Toughened composites*, Bandyopadhyay S, Gujjala R, CRC Press, pp.: 15-27 [\[CrossRef\]](#)
18. Alidadi-Shamsabadi M, Arefazar A, Shokoohi S (2020) Improvement in the synthesis and characterization of glycidyl methacrylate-grafted EPDM through melt free radical process. *Rubber Chem Technol* 93: 222-234 [\[CrossRef\]](#)
19. Shokoohi S, Arefazar A, Naderi G (2011) Compatibilized polypropylene/ethylene-propylene-diene-monomer/polyamide6 ternary blends: Effect of twin screw extruder processing parameters. *Mater Des* 32: 1697-1703 [\[CrossRef\]](#)
20. Al-Malaika S, Kong W (2005) Reactive processing of polymers: Functionalisation of ethylene-propylene diene terpolymer (EPDM) in the presence and absence of a co-agent and effect of functionalised EPDM on compatibilisation of poly(ethylene terephthalate)/EPDM blends. *Polym Degrad Stab* 90: 197-210 [\[CrossRef\]](#)
21. Li H, Sui X, Xie X (2018) Correlation of morphology evolution with superior mechanical properties in PA6/PS/PP/SEBS blends compatibilized by multi-phase compatibilizers. *Chinese J Polym Sci* 36: 848-858 [\[CrossRef\]](#)
22. Horiuchi S, Matchariyakul N, Yase K, Kitano T (1997) Morphology through an interfacial reaction in ternary immiscible polymer blends. *Macromolecules* 30: 3664-3670 [\[CrossRef\]](#)
23. Jazani OM, Arefazar A, Jafari SH, Beheshty MH, Ghaemi A (2011) A study on the effects of SEBS-g-MAH on the phase morphology and mechanical properties of polypropylene/polycarbonate/SEBS ternary polymer blends. *J Appl Polym Sci* 121: 2680-2687 [\[CrossRef\]](#)
24. Jazani OM, Arefazar A, Peymanfar MR, Saeb MR, Talaei A, Bahadori B (2013) The Influence of NBR-g-GMA compatibilizer on the morphology and mechanical properties of

- poly (ethylene terephthalate)/polycarbonate/NBR ternary blends. *Polym Plast Technol Eng* 52: 1295-1302 [\[CrossRef\]](#)
25. Luna CBB, Siqueira DD, da Silva Barbosa Ferreira E, Araújo EM, Wellen RMR (2020) Reactive compatibilization as a proper tool to improve PA6 toughness. *Mater Res Exp* 6: 125367 [\[CrossRef\]](#)
  26. Jazani OM, Arefazar A, Jafari SH, Peymanfar MR, Saeb MR, Talaei A (2013) SEBS-g-MAH as a reactive compatibilizer precursor for PP/PTT/SEBS ternary blends: Morphology and mechanical properties. *Polym Plast Technol Eng* 52: 206-212 [\[CrossRef\]](#)
  27. Delkash M, Naderi G, Sahraieyan R, Esmizadeh E (2017) Crystallization, structural and mechanical properties of PA6/PC/NBR ternary blends: effect of NBR-g-GMA compatibilizer and organoclay. *Sci Eng Compos Mater* 24: 669-678 [\[CrossRef\]](#)
  28. Codou A, Anstey A, Misra M, Mohanty AK (2018) Novel compatibilized nylon-based ternary blends with polypropylene and poly(lactic acid): morphology evolution and rheological behaviour. *RSC Adv* 8: 15709-15724 [\[CrossRef\]](#)
  29. Anstey A, Codou A, Misra M, Mohanty AK (2018) Novel compatibilized nylon-based ternary blends with polypropylene and poly(lactic acid): Fractionated crystallization phenomena and mechanical performance. *ACS Omega* 3: 2845-2854 [\[CrossRef\]](#)
  30. Mostofi N, Nazockdast H, Mohammadigoushki H (2009) Study on morphology and viscoelastic properties of PP/PET/SEBS ternary blend and their fibers. *J Appl Polym Sci* 114: 3737-3743 [\[CrossRef\]](#)
  31. Rastin H, Saeb MR, Jafari SH, Khonakdar HA, Kritschmar B, Wagenknecht U (2015) Reactive compatibilization of ternary polymer blends with core-shell type morphology. *Macromol Mater and Eng* 300: 86-98 [\[CrossRef\]](#)
  32. Mehrabi Mazidi M, Razavi Aghjeh MK (2015) Effects of blend composition and compatibilization on the melt rheology and phase morphology of binary and ternary PP/PA6/EPDM blends. *Polym Bull* 72: 1975-2000 [\[CrossRef\]](#)